Epilepsy Research 157 (2019) 106187

Contents lists available at ScienceDirect

Epilepsy Research

journal homepage: www.elsevier.com/locate/epilepsyres

Semi-automatic quantification of seizure-related effects on heart activity

Arthur Jordan[a,b,1], Marcel Bausch[a,1], Rainer Surges[a,*]

[a] Department of Epileptology, University Hospital Bonn, Bonn, Germany
[b] Department of Neurology, University Hospital of Aachen, Aachen, Germany

ARTICLE INFO

Keyword:
HR analysis

ABSTRACT

Objective: : Seizure-related modulation of heart rate (HR) was examined extensively in previous studies. However, the overall effect on HR attributable to epileptic seizures is difficult to determine, given the considerable fluctuations of HR before and during seizures. Here, we developed a semi-automatic procedure allowing quantification of the total impact of seizures on HR and determination of temporal relationships between seizure onset assessed by intracranial EEG (iEEG) and ECG.

Methods: : ECG and iEEG data of epilepsy patients undergoing video-EEG telemetry for epilepsy surgery with bilateral hippocampal depth electrodes were analysed retrospectively. Consecutive RR intervals and HR profiles were determined using R detection algorithms. Novel features including the normalized ictal area under the curve (niAUC), as well as the time point of ECG onset (HR breakpoint) were calculated. Selected HR features were compared to widely-used manually acquired measures. Data are given as median ± SD.

Results: : Fifteen patients had a total of 34 seizures with left-hippocampal and 37 seizures with right-hippocampal onset. HR increased by 9 ± 19% during seizures. Latency between iEEG seizure-onset to the HR breakpoint was 23 ± 22 s. No significant difference between left- and right-hippocampal seizures was observed with respect to HR increases, latencies and niAUC. A comparison between results of the semi-automatic and manual approach revealed that ictal HR changes showed a higher correlation (r = 0.6) than niAUC (r = 0.4).

Conclusions: : The proposed semi-automatic approach to analyze continuous HR data provides useful tools for estimating the overall effect of seizures on HR in greater detail. Our results suggest that the side of hippocampal seizure onset has no significant effect on the latency and extent of ictal HR changes. The algorithms may be of further use in clinical research and the development of seizure detection devices.

1. Introduction

Brain regions involved in the autonomic nervous system (ANS) can be affected during epileptic seizures, resulting in a variety of autonomic symptoms. Previous studies analysed features of HR with regard to their localizing and lateralizing value in people with epilepsy (Britton et al., 2006; Garcia et al., 2001; Kawai et al., 2006; Leutmezer et al., 2003; Moseley et al., 2011; Panchani et al., 2011). Ictal tachycardia (ITC) occurs frequently, either as a consequence of excessive movement or due to spread of seizure activity into regions of the central ANS. ITC appears to occur more frequently in seizures of temporal lobe origin (Garcia et al., 2001; Weil et al., 2005). Ictal bradycardia, albeit far less prevalent, is of greater clinical interest due to its hemodynamic consequences (Britton et al., 2006; Hampel et al., 2017; Reeves et al., 1996). Recent studies also examined temporal relationships between EEG seizure onsets and ECG changes with potential relevance for closed-loop intervention systems based on HR (Hirsch et al., 2015; Leutmezer et al., 2003).

Most previous studies have capitalized on threshold-based detection of seizure-related HR changes which are limited by the fact that this approach usually does not take the entire duration of the seizure into account. Moreover, individual thresholds are often selected arbitrarily for each seizure or patient despite the existence of established thresholds such as 100 bpm for ITC and 60 bpm for ictal bradycardia. In a recent study we investigated whether ictal HR modulation depends on the hemisphere of seizure-onset (Surges et al., 2013). Since a quantitative approach was required, we captured maximum deviations from a pre-ictal reference HR snapshot under the assumption that the maximal or minimal HR deflection from a pre-ictal baseline value adequately reflects the overall degree of influence the seizure has on cardiac action. Because of EMG and movement artifacts, HR was sampled manually ("manual max method"). Similar approaches were also chosen in

* Corresponding author at: Department of Neurology, University Hospital RWTH Aachen, Pauwelsstr. 30, 52074 Aachen, Germany.
E-mail address: ajordan@ukaachen.de (A. Jordan).

[1] These authors contributed equally to this work.

https://doi.org/10.1016/j.eplepsyres.2019.106187
Received 23 April 2019; Received in revised form 21 July 2019; Accepted 11 August 2019
Available online 12 August 2019

previous studies by other authors in epilepsy research as well as in treadmill exercise studies (Jouven et al., 2005; Nashef et al., 1996; Opherk et al., 2002; Zijlmans et al., 2002).

While the manual max method is a measure of the maximal extent to which HR is altered after seizure onset, it does not consider any other HR changes over the entire course of the seizure, which upon closer inspection often follow complex dynamics and therefore likely contain valuable information about the overall impact a seizure may have on the ANS. Here, we developed and applied novel measures of ictal HR analysis to characterize seizure-related effects on HR in greater detail. Furthermore, we analysed latencies between EEG seizure-onset to ECG breakpoint (Hirsch et al., 2015; Kato et al., 2014; Stefanidou et al., 2015).

2. Materials, methods and patient collective

2.1. Patients

Video-EEG data of patients with medically refractory mesial temporal lobe epilepsy undergoing presurgical video-EEG monitoring between January 2000 and December 2011 in the Department of Epileptology at the University Hospital Bonn (Germany) were reviewed retrospectively. Since this study is a retrospective audit of EEG and ECG data collected during clinical procedures, informed patient consent was not required. The study was approved as such by the local medical ethics committee (Ethikkommission an der Medizinischen Fakultät der Rheinischen Friedrich-Wilhelms-Universität Bonn). The patient group and electrophysiological data analysed in this study were already reported in one of our previous studies (Surges et al., 2013). All patients were implanted with bilateral hippocampal depth electrodes and had at least 2 recorded seizures with independent onset from each hippocampus. A summary of the clinical details is given in Table 1.

2.2. Manual EEG and ECG analysis

EEG data acquisition was performed with a Stellate Harmonie digital video-EEG system (Version 5.4, Schwarzer GmbH/Natus, Germany) using up to 128 channels, a 200 Hz sampling rate and a 16-bit analog-to-digital converter. Data were band pass filtered between 0.016 and 70 Hz. ECG recordings were acquired simultaneously with iEEG from a modified lead-I configuration. The main prerequisite for ictal HR analysis is the identification of iEEG seizure onset and propagation time of seizure activity to the contralateral hemisphere, which was done manually by reviewing iEEG data with particular focus on the bilateral hippocampal depth electrodes. The iEEG seizure onset separates the pre-ictal and ictal periods both for the manual and the semi-automatic method. The criteria for a typical seizure of hippocampal origin are onset with low amplitude fast activity (LAFA) or hypersynchronous discharges (Alarcon et al., 1995; Engel Jr, 2001) and the modulation of frequency and amplitude of the discharges as the seizure progresses. The occurrence of such ictal activity in the EEG electrodes of the contralateral hemisphere in the further course of the seizure was considered as propagation phenomenon, which was defined as the end of unilateral activity. The HR analysis was limited to the time interval before seizure onset until the time point of seizure propagation to the contralateral hemisphere. To rule out the influence of contralateral seizure activity on HR as accurately as possible, only the time interval between seizure onset and propagation was analysed whenever a propagation was present.

The objective of the manual max method was to get an estimate of the effect of seizure activity on the central ANS by measuring HR in ictal ECG recordings at predefined time points in a manual and therefore artifact-immune manner. In order to obtain the pre-ictal "baseline" value for the manual method, four consecutive RR intervals at a fixed one minute interval prior to seizure onset were measured within the Stellate Harmonie EEG analysis environment and their mean was calculated. For the ictal value the same approach was applied at the moment of maximum HR deviation from the pre-ictal value, which can be towards lower as well as towards higher HR. The maximum deviation was considered and chosen in order to normalize the recording and to allow comparison across all analysed seizures. In addition, the number of seizures during which HR exceeded 100 bpm (which is commonly defined as tachycardia) was determined. Another approach to explore effects of the EEG seizure onset on HR is to analyze ictal HR changes relative to individual baseline values. We therefore defined a significant HR increase as an increase of the ictal median HR of 2 SD above the pre-ictal median HR. This approach, however, requires a semi-automatic ECG analysis, which is described in the next section.

2.3. Semi-automatic ECG analysis

In order to obtain continuous HR profiles across the entire peri-ictal interval, all seizure recordings were exported in ASCII .txt format from the Stellate software and the ECG channels and analysed using custom MATLAB (version R2011a) scripts. Two different algorithms were used for R detection: the first one was developed by LIBROW™ (Chernenko, 2007) and the second one is a MATLAB implementation of the widely known Pan Tompkins algorithm (Sedghamiz, 2014). Results of both algorithms were compared manually for each seizure and results with greater number of outliers and distorted areas were rejected. Recordings that could not be assessed with either of the two algorithms due to insufficient signal to noise ratio (SNR) were discarded. Because of this manual review, this approach is referred to as "semi-automatic". A custom filter has been developed to remove artifacts and inaccuracies in the HR profiles, caused by motion and EMG noise in the underlying ECG data. Outliers in the HR profiles are detected by calculating the difference between each data point of the raw HR profile and its convoluted version and marking data points that lie outside the 1% bounds of the probability density function of these differences. The MATLAB code for the filter can be reviewed in the filterHRprofile function in the supplementary section.

These continuous HR profiles were used to calculate the pre-ictal baseline, median ictal HR, pre-ictal and ictal AUC as well as the latency to significant HR changes. The median of all instantaneous pre-ictal HR values (60/RR in seconds) prior to the seizure onset in iEEG constitutes the baseline. This baseline value is therefore not to be confused with the manually determined baseline. It is depicted as the grey horizontal line in Fig. 3. The median of all HR values during the time interval where seizure activity in iEEG is limited to the onset hemisphere constitutes the "automatic median value", which is shown in Fig. 3 as the purple (short) horizontal line. Medians were chosen because they are less sensitive to outliers caused by residual R detection artifacts. HR data in the time intervals after electroencephalographic spread of seizure activity to the contralateral hemisphere is less relevant for our lateralization analyses, however its relationship with the latency to seizure propagation was examined. For this analysis the median HR for the time interval between the propagation and seizure cessation was calculated. Seizures with a duration of less than 10 s prior to being detectable in the contralateral hemisphere were also discarded. In order to examine the amount of false positive HR increases we split the original baseline interval into two halves, the first of which we consider to represent the non-peri-ictal period and the second of which constitutes the immediate baseline interval (immediately preceding the seizure). A false positive HR increase is detected if in a dataset the median HR of the non-peri-ictal period exceeds 2 SD of the half of the baseline interval immediately preceding the seizure onset.

In order to calculate the normalized ictal AUC (niAUC) a continuous function for smoothening was approximated for each HR profile by convolving the HR data with a gaussian kernel and interpolating the data points removed by the artifact filter, by means of spline interpolation. The area between the smoothened HR graph and the pre-ictal baseline was calculated for a pre-ictal and ictal interval by means of

Table 1
Clinical details and analysed seizures of patients.

Patient no.	Sex	Age[*]/Epilepsy duration[*]/ handedness	MRI finding	Surgery	Intracranial electrodes	Seizure onset	Seizure type	Duration[+]
48	M	32/32/R	Bilat. HS	No	Hipp: 1 depth electrode (10 c.) on each side from posterior	Left-hippocampal	CPS	180 s
					ExHipp: None		SGTCS	184 s
						Right-hippocampal	CPS	113 s
							CPS	121 s
							CPS	154 s
105	M	39/3/R	Bilat. HS R > L	No	Hipp: 1 depth electrode (10 c.) on each side from posterior	Left-hippocampal	SPS[−]	118 s
					ExHipp: None		SPS[−]	132 s
						Right-hippocampal	SPS[−]	137 s
							SPS	75 s
							SPS	254 s
111	M	28/23/L	HS L	SAHE L	Hipp: 1 depth electrode (10 c.) on each side from posterior	Left-hippocampal	CPS	79 s
					ExHipp: 1 temporo-lateral (16 c.) and 2 temporo-basal (4 c.) strip electrodes on left side		CPS	120 s
							CPS	71 s
						Right-hippocampal	CPS	60 s
							CPS	37 s
							CPS	38 s
112	F	24/4/R	Bilat. HS L > R	No	Hipp: 1 depth electrode (10 c.) on each side from posterior	Left-hippocampal	CPS	66 s
					ExHipp: 1 temporo-lateral (4 c.) and 2 temporo-basal (4 c.) strip electrodes on each side		CPS	95 s
						Right-hippocampal	CPS	73 s
							CPS	87 s
							CPS	47 s
119	F	55/33/R	Bilat. HS L > R	SAHE R	Hipp: 1 depth electrode (10 c.) on each side from posterior	Left-hippocampal	SCP	65 s
					ExHipp: 1 temporo-lateral (6 c.) and 2 temporo-basal (4 c.) strip electrodes on each side		SCP[−]	68 s
						Right-hippocampal	SCP	144 s
							CPS	127 s
							CPS	200 s
							CPS	100 s
127	M	45/39/L	None	No	Hipp: 1 depth electrode (10 c.) on each side from posterior	Left-hippocampal	CPS	130 s
					ExHipp: 1 temporo-lateral (4 c.) and 2 temporo-basal (4 c.) strip electrodes on each side		CPS	71 s
						Right-hippocampal	CPS	180 s
							CPS	282 s
							CPS	96 s
							CPS	195 s
132	F	47/7/R	Bilat. HS	No	Hipp: 1 depth electrode (10 c.) on each side from posterior	Left-hippocampal	CPS	61 s
					ExHipp: None		CPS	87 s
						Right-hippocampal	CPS	91 s
							SPS[−]	78 s
							SPS[−]	64 s
							CPS[−]	132 s
135	F	46/33/R	HS R	SAHE R	Hipp: 1 depth electrode (10 c.) on each side from posterior	Left-hippocampal	SPS	42 s
					ExHipp: 1 temporo-lateral (6 c.) and 2 temporo-basal (4 c.) strip electrodes on each side	Right-hippocampal	SPS	47 s
							CPS	66 s
							CPS	64 s
							SPS	255 s
143	M	22/15/L	None	SAHE L	Hipp: 1 depth electrode (10 c.) on each side from posterior	Left-hippocampal	CPS	102 s
					ExHipp: 2 temporo-basal (4 c.) strip electrodes on each side		CPS	115 s
					1 temporo-lateral strip electrode (6 c.) on right side and 1 grid electrode (32 c.) on left side covering Wernicke's area	Right-hippocampal	CPS	67 s
							SGTCS	128 s
							CPS	77 s

(*continued on next page*)

Table 1 (*continued*)

Patient no.	Sex	Age*/Epilepsy duration*/ handedness	MRI finding	Surgery	Intracranial electrodes	Seizure onset	Seizure type	Duration+
144	F	35/30/R	Bilat. HS L > R	No	Hipp: 1 depth electrode (10 c.) on each side from posterior	Left-hippocampal	SPS	163 s
					ExHipp: None	Right-hippocampal	CPS	243 s
							SPS	141 s
							SPS	20 s
							SPS	289 s
160	F	31/30/R	Bilat. HS	TL-resection incl. AHE L	Hipp: 1 depth electrode (10 c.) on each side from posterior	Left-hippocampal	SPS/CPS#	101 s
					ExHipp: None	Right-hippocampal	CPS	120 s
							CPS	69 s
							CPS	137 s
182	F	34/14/R	Bilat. HS L > R	No	Hipp: 1 depth electrode (10 c.) on each side from posterior	Left-hippocampal	CPS	102 s
					ExHipp: None		SGTCS	118 s
						Right-hippocampal	CPS	104 s
							SCP-	30 s
							SCP-	35 s
							SGTCS	191 s
							SGTCS	196 s
184	F	28/25/L	HS R	No	Hipp: 2 depth electrodes (8 c.) on each side from lateral	Left-hippocampal	SPS/CPS#	60 s
					ExHipp: 2 temporo-basal (4 c.) strip electrodes on each side		CPS-	111 s
						Right-hippocampal	SPS	28 s
							SGTCS	273 s
							CPS	188 s
							SCP-	44 s
							SPS	80 s
187	F	31/29/R	Bilat. HS	No	Hipp: 1 depth electrode (10 c.) on each side from posterior	Left-hippocampal	CPS	391 s
					ExHipp: 1 temporo-lateral (6 c.) and 2 temporo-basal (4 c.) strip electrodes on each side		CPS	173 s
						Right-hippocampal	CPS	193 s
							SCP	118 s
							SCP	86 s
							SCP	65 s
202	M	28/15/R	HS L	No	Hipp: 5 depths electrodes (10 c.) on each side from lateral	Left-hippocampal	CPS	134 s
					ExHipp: 2 frontal strip electrodes (8 c.) on each side	Right-hippocampal	SGTCS	147 s
							CPS	188 s
							CPS	143 s

c, electrode contacts; ExHipp, extrahippocampal; Hipp, hippocampal; HS, hipppocampal sclerosis; L, left; R, right; SAHE, selective amygdala-hippocampectomie; TL, temporal lobe; CPS, complex-partial seizures; SGTCS, secondarily generalized tonic-clonic seizure; SCP, subclinical EEG pattern (no objective clinical signs apart from alterations of cardiac activity and with or without testing); SPS, simple partial seizure.

* At telemetry.

\+ According to EEG pattern.

\# Consciousness not tested.

\- Excluded from semiautomatic analysis due to insufficient signal-to-noise-ratio.

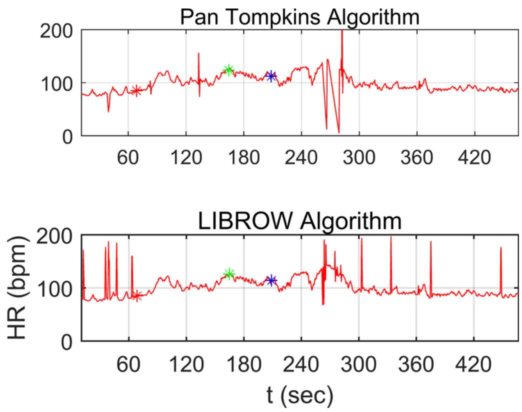

Fig. 1. R detection algorithms differently perform with ECG recordings containing artifacts. In this case, the result of the LIBROW algorithm was chosen and processed further. A left hippocampal seizure, recorded on patient 187 (as in Figure 3 and 2 D). The asterisks mark relevant timepoints, as assessed by EEG review. Red – beginning of unilateral seizure activity, green – propagation to the contralateral hemisphere, blue – cessation of the seizure.

trapezoidal numerical integration as implemented in MATLAB's trapz function. The ictal AUC is the area in the time interval between the seizure onset in iEEG and seizure cessation or spread to the contralateral hemisphere. This exact measure is visualized in Fig. 3 as the red area. The pre-ictal AUC (not shown in Fig. 3) constitutes the area under the smoothened HR graph and the pre-ictal baseline but for a time interval of equal length to the ictal interval to normalize for time. Its ending is marked by the iEEG seizure onset. The pre-ictal AUC was subtracted from the ictal AUC to obtain the final niAUC value, which is higher in case pre-ictal HR is below baseline HR and lower in case pre-ictal HR is higher than the baseline. niAUC therefore represents the effect of the EEG seizure onset on HR and is at the same time a measure for the cumulative effect on unilateral seizure activity on HR.

Computation of the HR breakpoint was accomplished by a novel statistical algorithm which detects HR increases greater than 1 SD above the pre-ictal baseline and with certain duration over a minimal time interval. This minimal time interval is also derived from the pre-ictal HR data by determining the number of consecutive values being greater than 1 SD. After random permutation of all pre-ictal instantaneous HR values, this process is repeated 10.000 times. Finally, the length of the largest of 10.000 "snippets" of consecutive HR values greater than 1 SD constitutes this minimal time interval. The beginning of the minimal time interval is defined as the ECG or HR breakpoint. The MATLAB code was made available in the calculateOnset function in the supplementary section.

2.4. Statistics

The distribution of the data was tested using the one-sample Kolmogorov-Smirnov test. For calculation of p-values in the lateralization analysis, a two-sided Wilcoxon rank sum test was performed, and data are given as medians ± SD and visualized as medians ± S.E.M. P values < 0.05 were considered statistically significant. MATLAB (versions R2011a and R2016b) was used to implement both the statistical analysis, as well as data visualisation.

3. Results

In 15 patients, 11 seizures out of a total of 82 had to be discarded entirely due to low SNR. Thirty-four left-sided and 37 right-sided hippocampal seizures were of sufficient signal quality to undergo further analysis. The performance of the two different R detection algorithms differed considerably when ECG artifacts were present in the recordings (Fig. 1). Overall, the LIBROW algorithm has proven to be more robust in analyzing the given datasets, failing to provide superior HR profiles in 3 seizures only, whereas the Pan Tompkins algorithm failed to deliver correct ECG analysis results in 9 seizures.

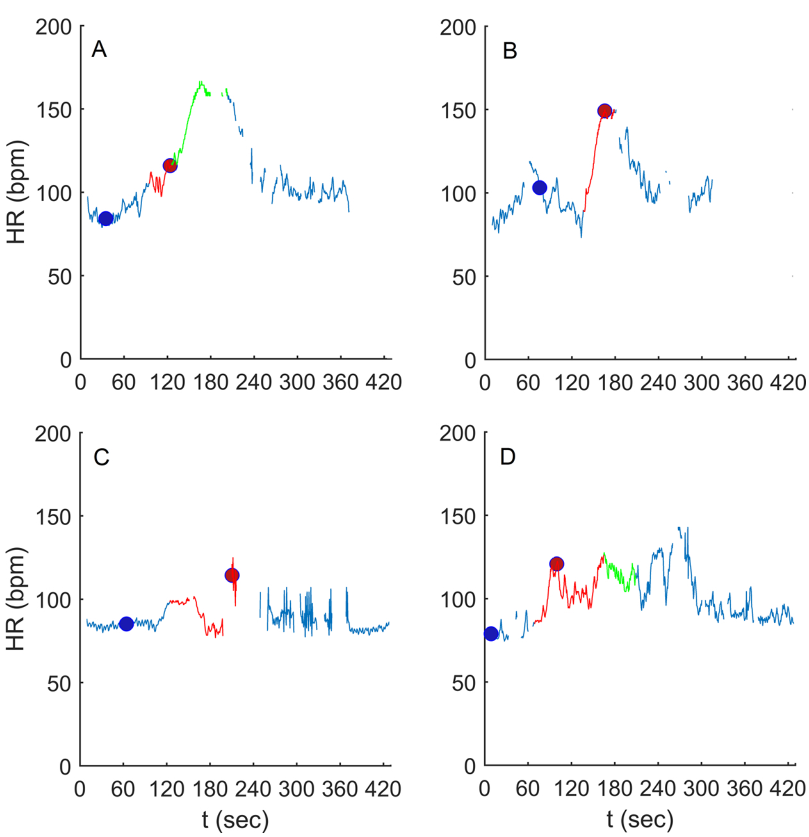

Fig. 2. Peri-ictal heart rate in temporal lobe epilepsy shows strong intraindividual as well as interindividual fluctuations. Automatic data after artifact removal, plotted alongside with the according manual data. Red graph: seizure activity limited to side of onset. Green graph: seizure activity propagated to the contralateral hemisphere. Blue circle: manual pre-ictal measurement. Red circle: manual ictal max measurement. **(A)** Patient 111, left-hippocampal seizure: steady increase in HR, which precedes EEG seizure onset. **(B)** Patient 111, right-hippocampal seizure without propagation to the contralateral electrodes with significant pre-ictal HR fluctuations. **(C)** Patient 202, left-hippocampal seizure without propagation with HR decrease. Residual artifacts are present. **(D)** Patient 187, left-hippocampal seizure with step-wise HR increase.

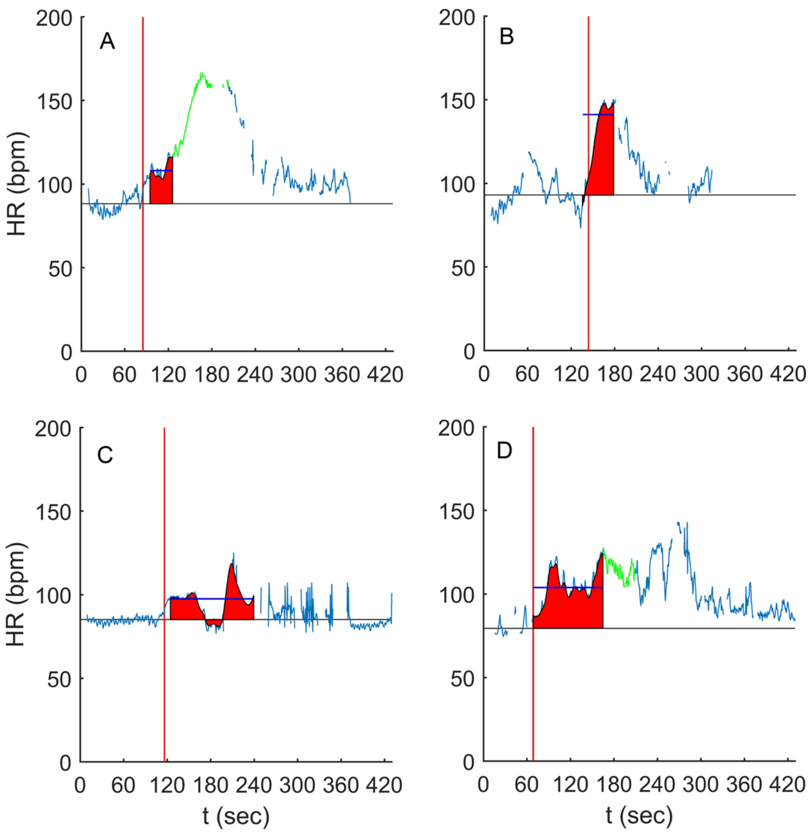

Fig. 3. Summary of all HR features, applied to the examples from Figure 2. Vertical red line: HR breakpoint, as calculated by the novel algorithm. Grey horizontal line: median pre-ictal HR (baseline). Red area: ictal AUC, calculated for the entire unilateral ictal interval under the spline interpolated (smoothened) curve. Seizure onset as determined by EEG is marked by the left bound of the red AUC. The right bound of the red AUC marks seizure cessation or propagation to the contralateral hemisphere (also beginning of the green graph). Purple (short) horizontal line: unilateral ictal HR median. Note: in **(A)** and **(C)** the HR breakpoint, as calculated by the HR breakpoint detection algorithm, precedes the EEG onset.

Importantly, hippocampal seizures display a very variable HR over time (Fig. 2). The semi-automatic analysis revealed local maxima and minima in the HR profile throughout the ictal period as well as during the pre-ictal phase in all seizures. Likewise, the duration of unilateral seizure activity shows a great variability (58 ± 63 s, range: 10–230 s). These results suggest that a more detailed semi-automatic analysis is superior to a manual investigation of seizure-related HR changes by selecting near-instantaneous HR derived from 4 consecutive RR intervals only. A semi-automatic analysis also allows determination of various other features.

A summary of novel peri-ictal HR features, as applied to the HR profiles is shown in Figure 3. The median of all pre-ictal HR values serves as a solid baseline allowing normalization of ictal AUC and relative ictal HR changes (see Fig. 3, horizontal lines). Furthermore, the HR breakpoint detection algorithm has proven to be very reliable in detecting significant HR changes (see Fig. 3, vertical red lines). The automatically detected HR breakpoint was delayed by 16 ± 22 s as compared to EEG seizure onset (Fig. 3 B), whereas in some seizures, the HR breakpoint preceded the EEG onset (Figs. 3 A and C). In 9 seizures, the latency from EEG seizure onset to HR breakpoint was greater than the duration of unilateral seizure activity. These seizures were excluded from the latency analysis.

In a next step, we investigated whether seizures with left-hippocampal onset were different from seizures with right-hippocampal onset with respect to these novel ECG features. In 91% of left-hippocampal and 70% of right-hippocampal seizures, HR transiently exceeded 100 bpm while still being limited to the onset hemisphere which might suggest that ictal tachycardia is more common in left-hippocampal seizures. However, in 21% (n = 7) of left and 28% (n = 9) of right hippocampal seizures HR exceeded 100 bpm throughout the pre-ictal interval. Fifty percent of left-sided and 54% of right-sided seizures displayed a significant heart rate increase of 2 SD above pre-ictal baseline. Six out of 71 seizures exhibited such false positive increases in HR and less than 10% of heart beats fell outside 2 SD of the immediate baseline interval (Supplementary Figure 3). Among simple partial seizures (SPS) the percentage of significant HR increases was the lowest (25 and 41% for left and right respectively) and among secondary generalized tonic-clonic seizures 67 vs. 75% displayed a significant increase (Supplementary Figure 1). No significant difference between left and right onset seizures was found (p = 0,24). No cases of ictal bradycardia (i.e. HR < 60 bpm or HR lower than 2 SD below the pre-ictal median) were observed. Fifty-four seizures occurred at daytime and 17 have been recorded during nocturnal period. We can observe a significant difference in baseline HR during nighttime (71.4 bpm ± 14 vs. 85.3 bpm ± 14), which was defined as the time period between 10:00 p.m. to 6:00 a.m. (p = 0.0017). No significant difference in absolute HR increase (11bpm ± 12 vs. 8bpm ± 13, p = 0.24) was observed between night and day (Supplementary Figure 2). In total 37 (21 left and 16 right-hemispheric onset) seizures propagated to the contralateral hemisphere. The median duration until propagation was 42 s (± 38 s Range 10–213 s). The median HR after propagation was 125 bpm (± 21 bpm range: 78–164 bpm). Median post-propagation HR was 124 bpm for left-sided and 140 bpm for right-sided seizures. Over all seizures the absolute change of post-propagation HR compared to the pre-ictal baseline shows a weak positive correlation (r = 0.0789, p = 0.6426) to the duration until seizure propagation occurs. Similarly, the correlation between the duration until seizure propagation and the median HR during unilateral seizure activity is non-significant (r = 0.0903, p = 0.5950). A comparison of pre-ictal and ictal HR values in left and right hippocampal seizures from the automatically computed data over the entire time intervals, as in manual measurements, revealed no significant lateralization effect (p = 0.95 and p = 0.55, Fig. 4 A). Comparisons of neither normalized ictal AUC nor latencies to seizure onset revealed significant differences between seizures with right and left-hippocampal onset (p = 0.92 and p = 0.58, Fig. 4 B and C). Surprisingly, increases of HR determined by the HR breakpoint detection algorithm preceded the apparent EEG seizure onset in 24% (n = 9, 8.5 ± 2.9 s) of left hippocampal seizures and in 11% (n = 4,

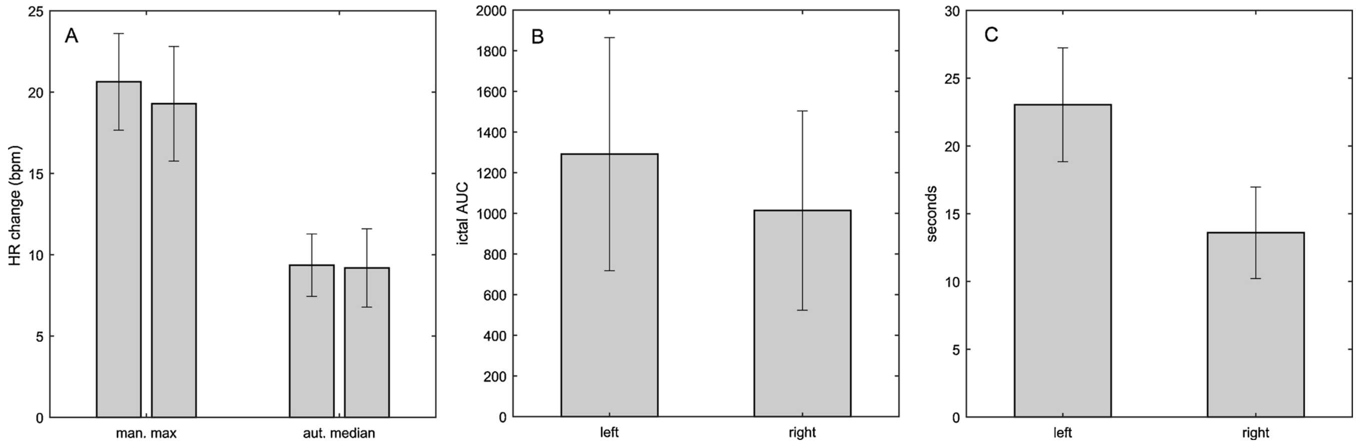

Fig. 4. Analysis of hemispheric lateralization. No significant lateralization effects are evident in any of the described HR features in the underlying data. Each bar represents the median of the underlying HR feature values across 34 left or 37 right onset hippocampal seizures ± S.E.M. **(A)** Comparison of the manual max method with the automatically calculated median across all ictal HR values. As expected, median max values are higher, however they fail to represent the time variable and can induce artificial effects. **(B)** Comparison of median niAUC in left vs. right-hippocampal seizures. **(C)** Comparison of latencies between iEEG seizure onset and the HR breakpoint, as calculated by the breakpoint detection algorithm.

4.7 ± 1.9 s) of right hippocampal seizures. Out of 12 seizures with HR breakpoints preceding the iEEG onset we found 1 seizure with 2/s slow waves in the corresponding hippocampal depth electrodes, whereas the rest featured either LAFA (n = 1) or hypersynchronous spikes (n = 11). Irregular iEEG patterns are not over-represented among seizures with premature HR breakpoints.

Finally, we compared the characteristics of the manually determined seizure-related HR to ECG features extracted by semi-automatic analysis. While the manual max method appears to be reasonably well-suited for determination of the median ictal HR (Fig. 5 A, r = 0.6), it does not reliably predict the niAUC (r = 0.4) (Fig. 5 B).

4. Discussion

The aims of this study were to develop a more objective, accurate and precise approach for seizure-related HR analysis and to apply it to continuous HR data recorded in a highly selected patient group to test the value of HR as a lateralizing sign in TLE.

4.1. Methodical considerations

As a baseline for the manual max method, one pre-ictal snapshot was chosen at a fixed time point. Pre-ictal HR can display significant fluctuations, thereby distorting the baseline. Due to the short time interval being sampled, no accurate estimation of pre-ictal HR variability is possible. Moreover, our results show that several HR maxima can be present throughout the course of the seizure. In some studies, besides maximal HR deflections from the baseline, several HR samples were taken at fixed time points, which might account for ictal HR fluctuations to a better degree (Garcia et al., 2001; Moseley et al., 2011). Median ictal and pre-ictal HR are features which incorporate all pre-ictal and ictal RR intervals, which represent, at least to some extent, the

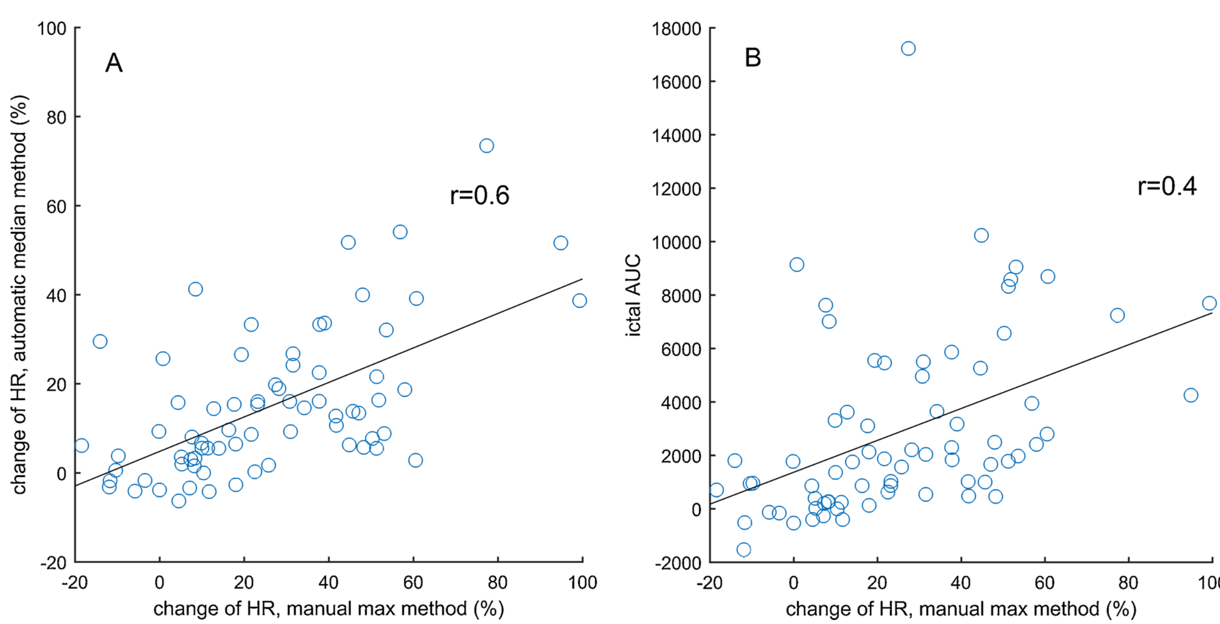

Fig. 5. Taking “HR snapshots” correlates less to niAUC than to the median ictal HR. **(A)** Each data point represents the relative HR change in the manual max method as well as the automatic median method. A significant correlation is to be expected here. **(B)** Correlation of the niAUC with the relative HR change in the manual max method. With the time variable having a greater influence on the ictal AUC, the correlation with the manual “snapshots” becomes less pronounced.

variability over time and which are rather robust against artifacts. Therefore, we decided to include this rather conservative feature into our analyses as a reference. A better representation of the time variable is achieved by calculating niAUC. Ictal AUC without the normalization would constitute a measure for the total amount of additional heartbeats induced by seizures. The normalization considers HR changes shortly before iEEG seizure onset and therefore corrects for them, resulting in the niAUC, which reflects the HR changes taking place solely due to iEEG seizure onset. We also addressed the question how well niAUC and relative HR changes as assessed by the novel semi-automatic approach are predicted by the manual max method. The correlations (Fig. 5) show that niAUC is less well predicted by the manual approach, suggesting that the manual approach fails to give a sufficient estimate of the total impact that seizures exert on HR.

Pronounced alterations of HR during seizures may be of great clinical interest, as ictal bradycardia can progress into asystole (Devinsky, 2004; Schuele et al., 2007) and ITC can be accompanied by altered atrioventricular conduction as well as atrial and ventricular extrasystoles, possibly raising the risk for fatal arrhythmia (22–24). ITC is commonly defined as HR greater than 100 (Hirsch et al., 2015) or 120 bpm (Britton et al., 2006), HR increases greater than 20% (Hirsch et al., 2015; Stefanidou et al., 2015) or HR being greater than the 98th percentile (Moseley et al., 2011). Leutmezer et al. defined ITC as HR being greater than 1 SD of median pre-ictal HR of all patients in the considered group. Our results show that artificial effects can result from choosing different ITC definitions. Since peri-ictal HR shows intra-individual as well as inter-individual variability which must be accounted for, we would consider the 98th percentile or 2 SD definition of ITC as the most suitable for future studies. For the overwhelming majority of seizures less than 10% of heart beats fell outside 2 SD of the immediate baseline interval. Unfortunately the available datasets only represented the peri-ictal period which only had an overall duration in the order of a few minutes. While this data is suitable for examining several aspects of HR dynamics shortly before, during and after a seizure onset and addressing the question of an asymmetrical representation of peri-ictal HR modulation, it cannot show how often the HR falsely exceeded 2 SD of a floating baseline calculated well outside of the ictal/immediate pre-ictal period. For the development of seizure detection systems based on HR dynamics knowing this false positive rate of tachycardia detections is crucial, since a high number of false alarms would not be acceptable to most patients and caregivers. Including accelerometry data might help to differentiate between ictal HR increases and HR increases due to physical activity. In our patient collective, we also observed a correlation of HR with clinical severity of the seizure (SPS vs. CPS vs. GTCS) which was to be expected. No significant difference in absolute HR increase was observed between night and day suggesting that sleep-wake-cycles do not modulate the influence of seizures on HR.

In view of variable nature of peri-ictal HR, analysis of continuous HR data is necessary. Using two different R detection algorithms can increase the number of successfully analysed ECG datasets due to individual strengths and weaknesses of each algorithm. In most of our datasets, filtering of the HR profiles was required. Interpolation of the resulting “gaps” by means of spline interpolation was mandatory for calculating the niAUC, since a continuous function is necessary for trapezoidal numerical integration. These two steps can be omitted if HR profiles do not contain noteworthy amounts of artifacts. Calculation of pre-ictal and ictal median HR does not require interpolation.

To our knowledge, this study is the first to assess niAUC in HR profiles. Leutmezer and colleagues investigated HR dynamics with respect to the EEG seizure onset and found that HR at the time of seizure onset typically displays two ways of rising (Leutmezer et al., 2003). Our data suggest that in the further course of the seizure, HR dynamics vary to a greater extent. Several different patterns, as depicted in Figs. 2 and 3, are possible. In some cases, HR decreases after an initial increase (Figure 3 and 2 C) or shows a step-wise increase (Figure 3 and 2 D). niAUC represents these variations, however caution is advised with ECG data with low SNR. Excessive amounts of artifacts in the resulting HR profiles, as well as large spline interpolated intervals can distort the integrals. HR breakpoints in peri-ictal HR profiles were determined in previous studies with different techniques (Di Gennaro et al., 2004; Leutmezer et al., 2003; Van Elmpt et al., 2006; Kato et al., 2014). The present semi-automatic approach based on MATLAB algorithms provides additional helpful tools, which iare provided as open source files.

In summary, a thorough analysis of continuous HR profiles adds to our understanding of seizure-related HR modulation. This step allows for quantification of peri-ictal as well as ictal fluctuations, calculation of mean or median HR over greater time intervals and finally makes the calculation of features such as HR breakpoint and niAUC possible. While HR breakpoints make latency measurements possible, niAUC is a measure of the cumulative effect of seizure activity on HR and thereby directly or indirectly on the central ANS.

4.2 Does modulation of HR depend on the hemisphere of seizure-onset?

In our highly selected patient group with seizures independently arising from hippocampi of both hemispheres, we did not observe differences on any HR feature irrespective of the applied method. Our findings are in line with a number of previous studies, suggesting that the side of seizure-onset does not influence peri-ictal HR modulation (Epstein et al., 1992; Garcia et al., 2001; Hampel et al., 2017; Keilson et al., 1987; Moseley et al., 2011; Opherk et al., 2002; Rugg-Gunn et al., 2004; Schernthaner et al., 1999), while other studies found evidence for asymmetric effects depending on the hemisphere (Jouven et al., 2005; Kawai et al., 2006).

Di Gennaro et al. investigated latencies from surface EEG onset to HR changes in seizures of temporal lobe origin, reporting no significant difference between left and right (Di Gennaro et al., 2004). Kato and colleagues performed a study suggesting that right mesial temporal lobe seizures have earlier tachycardia onsets (Kato et al., 2014). A similar approach of detecting the HR breakpoint as in our study was applied. However, the EEG seizure onsets in their investigation were detected using surface EEG and the patient group only included patients with seizures arising in one hemisphere. Hirsch et al. analyzed temporal relationships between the seizure onset of ITC, defined as either HR greater than 100 bpm or 20% of a baseline value (Hirsch et al., 2015). They reported longer latencies to ITC in left-hemispheric seizures, however, with an underrepresentation of right-hemispheric seizures. In their collective ictal tachycardia never preceded the iEEG seizure onset. Stefanidou et al. performed an intracranial EEG study, showing that laterality at seizure onset did not predict the occurrence of ITC and that bilateral seizure onset is associated with early tachycardia (Stefanidou et al., 2015).

In our patient group, each patient had seizures arising from both hemispheres independently and the seizure onsets were detected from hippocampal depth electrodes. Importantly, we included 34 left-hippocampal and 37 right-hippocampal seizures in our analysis, which is a well-balanced ratio of right to left and we ruled out influences of the contralateral hemisphere as accurately as possible. We did not observe significant hemisphere-differential effects on latency to the HR breakpoint. The median latency in right-onset seizures appeared to be slightly shorter as compared to left-onset seizures, but the HR breakpoint preceded the apparent seizure-onset as assessed by iEEG in a greater proportion of left-onset seizures. The observation that HR started to rise before apparent electroencephalographic seizure onset might be explained with inaccuracies in iEEG seizure-onset detection caused by subjective bias of the examiners, spatial sampling bias of the limited number of intracranial EEG electrodes or by inaccurate determination of the HR breakpoint. We do not regard the fact that in the study by Hirsch et al. ictal tachycardia was never observed prior to iEEG seizure onsets as a contradiction to our results, because the HR breakpoint is a phenomenon that usually occurs before HR reaches 100bpm or 20% HR increase above baseline. In view of most previous studies and our present results, we believe that the temporal relationships between (i)

EEG seizure onset and HR breakpoint as well as the magnitude of HR changes are of little use as a lateralizing sign in temporal lobe epilepsy and that a putative hemispherical effect, if present, is not clinically meaningful.

5. Conclusions

We have developed a novel MATLAB based approach which allows a semi-automatic analysis of the total impact of seizures on HR and provides novel HR features that may be useful in future automatic seizure detection techniques based on HR measurements. The main analytical methods have been made public in the form of MATLAB script files. The time course of HR during temporal lobe seizures arising from the hippocampus is very variable and does not depend on the side of seizure-onset.

Funding

This research did not receive any specific grant from funding agencies in the public, commercial, or not-for-profit sectors.

Declaration of Competing Interest

A. Jordan and M. Bausch have no financial disclosure to make. R. Surges has received speaker fees or honorary for serving on the advisory board from Bial, Cyberonics, Desitin, Eisai, LivaNova, Novartis and UCB Pharma.

Appendix A. Supplementary data

Supplementary material related to this article can be found, in the online version, at doi:https://doi.org/10.1016/j.eplepsyres.2019.106187.

References

Alarcon, G., Binnie, C.D., Elwes, R.D.C., Polkey, C.E., 1995. Power spectrum and intracranial EEG patterns at seizure onset in partial epilepsy. Electroencephalogr. Clin. Neurophysiol. 94, 326–337.
Britton, J.W., Ghearing, G.R., Benarroch, E.E., Cascino, G.D., 2006. The ictal bradycardia syndrome: localization and lateralization. Epilepsia 47, 737–744.
Chernenko, S., 2007. ECG Processing — R-peaks Detection — Librow — Software [WWW Document]. http://www.librow.com/cases/case-2.
Devinsky, O., 2004. Effects of seizures on autonomic and cardiovascular function. Epilepsy Curr. 4, 43–46.
Di Gennaro, G., Quarato, P.P., Sebastiano, F., Esposito, V., Onorati, P., Grammaldo, L.G., Meldolesi, G.N., Mascia, A., Falco, C., Scoppetta, C., 2004. Ictal heart rate increase precedes EEG discharge in drug-resistant mesial temporal lobe seizures. Clin. Neurophysiol. 115, 1169–1177.
Engel Jr, J., 2001. Mesial temporal lobe epilepsy: what have we learned? Neuroscientist 7, 340–352.
Epstein, M.A., Sperling, M.R., O'connor, M.J., 1992. Cardiac rhythm during temporal lobe seizures. Neurology 42, 50.
Garcia, M., D'Giano, C., Estelles, S., Leiguarda, R., Rabinowicz, A., 2001. Ictal tachycardia: its discriminating potential between temporal and extratemporal seizure foci. Seizure 10, 415–419.
Hampel, K.G., Thijs, R.D., Elger, C.E., Surges, R., 2017. Recurrence risk of ictal asystole in epilepsy. Neurology 10.1212/WNL. 0000000000004266.
Hirsch, M., Altenmüller, D.-M., Schulze-Bonhage, A., 2015. Latencies from intracranial seizure onset to ictal tachycardia: a comparison to surface EEG patterns and other clinical signs. Epilepsia 56, 1639–1647.
Jouven, X., Empana, J.-P., Schwartz, P.J., Desnos, M., Courbon, D., Ducimetière, P., 2005. Heart-rate profile during exercise as a predictor of sudden death. N. Engl. J. Med. 352, 1951–1958.
Kato, K., Jin, K., Itabashi, H., Iwasaki, M., Kakisaka, Y., Aoki, M., Nakasato, N., 2014. Earlier tachycardia onset in right than left mesial temporal lobe seizures. Neurology 83, 1332–1336.
Kawai, M., Goldsmith, I.L., Verma, A., 2006. Differential effects of left and right hemispheric seizure onset on heart rate. Neurology 66, 1279–1280. https://doi.org/10.1212/01.wnl.0000208519.40986.fb.
Keilson, M.J., Hauser, W.A., Magrill, J.P., Goldman, M., 1987. ECG abnormalities in patients with epilepsy. Neurology 37, 1624.
Leutmezer, F., Schernthaner, C., Lurger, S., Pötzelberger, K., Baumgartner, C., 2003. Electrocardiographic changes at the onset of epileptic seizures. Epilepsia 44, 348–354.
Moseley, B.D., Wirrell, E.C., Nickels, K., Johnson, J.N., Ackerman, M.J., Britton, J., 2011. Electrocardiographic and oximetric changes during partial complex and generalized seizures. Epilepsy Res. 95, 237–245.
Nashef, L., Walker, F., Allen, P., Sander, J.W., Shorvon, S.D., Fish, D.R., 1996. Apnoea and bradycardia during epileptic seizures: relation to sudden death in epilepsy. J. Neurol. Neurosurg. Psychiatry 60, 297–300.
Opherk, C., Coromilas, J., Hirsch, L.J., 2002. Heart rate and EKG changes in 102 seizures: analysis of influencing factors. Epilepsy Res. 52, 117–127.
Panchani, J., Adjei, P., Henneberger, C., Scott, C.A., Thompson, A.J., Diehl, B., Walker, M.C., Surges, R., 2011. Asymmetric hemispheric representation of periictal heart rate modulation is individually lateralised. Epileptic Disord. 13, 172–176.
Reeves, A.L., Nollet, K.E., Klass, D.W., Sharbrough, F.W., So, E.L., 1996. The ictal bradycardia syndrome. Epilepsia 37, 983–987.
Rugg-Gunn, F.J., Simister, R.J., Squirrell, M., Holdright, D.R., Duncan, J.S., 2004. Cardiac arrhythmias in focal epilepsy: a prospective long-term study. Lancet 364, 2212–2219.
Schernthaner, C., Lindinger, G., Pötzelberger, K., Zeiler, K., Baumgartner, C., 1999. Autonomic epilepsy–the influence of epileptic discharges on heart rate and rhythm. Wien. Klin. Wochenschr. 111, 392–401.
Schuele, S.U., Bermeo, A.C., Alexopoulos, A.V., Locatelli, E.R., Burgess, R.C., Dinner, D.S., Foldvary-Schaefer, N., 2007. Video-electrographic and clinical features in patients with ictal asystole. Neurology 69, 434–441.
Sedghamiz, H., 2014. Complete Pan Tompkins Implementation ECG QRS Detector - File Exchange - MATLAB Central [WWW Document]. http://de.mathworks.com/matlabcentral/fileexchange/45840-complete-pan-tompkins-implementation-ecg-qrs-detector.
Stefanidou, M., Carlson, C., Friedman, D., 2015. The relationship between seizure onset zone and ictal tachycardia: an intracranial EEG study. Clin. Neurophysiol. 126, 2255–2260.
Surges, R., Jordan, A., Elger, C.E., 2013. Ictal modulation of cardiac repolarization, but not of heart rate, is lateralized in mesial temporal lobe epilepsy. PLoS One 8, e64765.
Van Elmpt, W.J., Nijsen, T.M., Griep, P.A., Arends, J.B., 2006. A model of heart rate changes to detect seizures in severe epilepsy. Seizure 15, 366–375.
Weil, S., Arnold, S., Eisensehr, I., Noachtar, S., 2005. Heart rate increase in otherwise subclinical seizures is different in temporal versus extratemporal seizure onset: support for temporal lobe autonomic influence. Epileptic Disord. Int. Epilepsy J. Videotape 7, 199–204.
Zijlmans, M., Flanagan, D., Gotman, J., 2002. Heart rate changes and ECG abnormalities during epileptic seizures: prevalence and definition of an objective clinical sign. Epilepsia 43, 847–854.